Basic ideas and applications of the method of reduction of dimensionality in contact mechanics

V.L. Popov*

Berlin University of Technology, Berlin, 10623, Germany

The method of reduction of dimensionality in contact mechanics is based on a mapping of some classes of three-dimensional contact problems onto one-dimensional contacts with elastic foundations. Recently, a rigorous mathematical proof of the method has been provided for contacts of arbitrary bodies of revolution with and without adhesion. The method of reduction of dimensionality has been further verified for randomly rough surfaces. The present paper gives an overview of the physical foundations of the method and of its applications to elastic and viscoelastic contacts with adhesion and friction. Both normal and tangential contact problems are discussed.

Keywords: method of reduction of dimensionality, contact problem, adhesive contact, friction coefficient

DOI: 10.1134/S1029959912030022

1. Introduction

Computer simulations have been an integral part of the technical development process for a long time now. Tribology is one of the last fields in which computer simulations have, until now, played no significant role. This is primarily due to the fact that investigating tribological phenomena requires considering all spatial scales down to the microscales [1–3]. The current processing speeds of modern computers are not by far sufficient to simulate contact and friction phenomena for real surfaces while considering all relevant scales. Therefore, it is important to search for simulation methods which accept the loss of information about parts of the system, however, allow for a small number of especially meaningful macroscopic quantities to be quickly calculated. This technique is, of course, in no way new and is actually the tried and true method that science has followed since its inception. In the field of contact mechanics for real surfaces, one such possibility is presented, the method of reduction of dimensionality, which was first suggested in [4]. This method is based on the observation that close analogies exist between certain types of three-dimensional contact problems and the simplest contacts with a one-dimensional elastic foundation. Thereby, it is important to emphasize that this is not an approximation: The properties of one-dimensional systems coincide exactly with those of the original three-dimensional system. The price for this reduction is high, but for many applications quite acceptable. One obtains the exact results only for the relationships between the force, the (macroscopic) relative displacement of the bodies, and the contact radius. With this, all quantities that depend on the force-displacement relationship can be calculated. In the area of exact agreement, parameters such as the contact stiffness and the corresponding electrical resistance and thermal conductivity can be found. In the case of elastomers, dissipated energy and friction forces also belong to this set.

2. Basic ideas

We limit our consideration to "typical tribological systems" which are characterized by the laws of dry friction being approximately met, especially, the fact that the frictional force is approximately proportional to the normal force. This implies that the real contact area remains much smaller than the apparent contact area. For "typical tribological systems", there is a series of properties that allow for immense simplification of the contact problem and in this way, allow quick calculation even in multi-scaled systems. The simplifying properties used in the reduction method are the following [3]:

(i) for velocities much smaller than the speed of sound, deformations can be treated as quasi-static;

(ii) the potential energy, and therefore, the force-displacement relation, is a local property that depends only on the configuration of the microcontacts and not the form or size of the body;

(iii) the kinetic energy, on the other hand, is a "global property" that depends only on the form and size of the body as a whole and not on the configuration of the microcontacts.

* *Corresponding author*
Prof. Valentin L. Popov, e-mail: v.popov@tu-berlin.de

The last two properties mean that the "elastic properties" and the "inertia properties" are completely decoupled, the first being purely microscopic and the latter, purely macroscopic. The above three properties are found in many macroscopic tribological systems. The application area of the subsequent methods is, accordingly, very wide.

Another crucial property of contacts between three-dimensional bodies is the close similarity between these contacts and certain one-dimensional problems. The fundamental ideas of this analogy are presented in the following. If a cylindrical indenter is pressed into the surface of an elastic continuum (Fig. 1, *a*), then the stiffness k of the contact is proportional to its diameter D [3]:

$$k = DE^*, \tag{1}$$

where E^* is the effective elastic modulus:

$$\frac{1}{E^*} = \frac{1-\nu_1^2}{E_1} + \frac{1-\nu_2^2}{E_2}, \tag{2}$$

E_1 and E_2 are the Young's moduli of contacting bodies, and ν_1 and ν_2, their Poisson ratios. The proportionality of the stiffness to the diameter can be reproduced using a one-dimensional elastic foundation (Fig. 1, *b*). In order to fulfill Eq. (1), the stiffness per unit length must be chosen as E^*. Every individual spring must have the stiffness

$$\Delta k_z = E^* \Delta x, \tag{3}$$

where Δx is the distance between the springs of the elastic foundation and z is the vertical coordinate.

The tangential stiffness of a three-dimensional contact is also proportional to the diameter of the contact [3]:

$$k_x \approx DG^*, \tag{4}$$

where

$$\frac{1}{G^*} = \frac{2-\nu_1}{4G_1} + \frac{2-\nu_2}{4G_2}, \tag{5}$$

G_1 and G_2 are the shear moduli of contacting bodies. For the same reasons as in the case of a normal contact, the tangential contact can be replicated using a one-dimensional elastic foundation. The tangential stiffness of individual springs in the elastic foundation must be chosen according to

$$\Delta k_x = G^* \Delta x. \tag{6}$$

3. The Geike–Popov rule and the Hess rule for normal contacts

Amazingly, the contact with an elastic foundation defined with (3) gives correct force-displacement relations not only for cylindrical indenters but also for a large class of simple surface profiles. However, the surface profile must be modified according to some simple rules. For parabolic (or spherical) profiles, the rule was given by Geike and Popov [5]. They have shown that the relations between force, indentation depth and contact radius of a spherical indenter with radius R pressed into a half-space (Fig. 2, *a*) can be reproduced exactly with a contact with a one-dimensional elastic foundation (Fig. 2, *b*) by changing the radius. If a "sphere" with the radius R_1 is brought into contact with the elastic foundation (penetration depth d), then the following contact quantities result: The contact radius is equal to

$$a = \sqrt{2R_1 d} \tag{7}$$

and the normal force is

$$F_N(d) = \frac{4\sqrt{2}E^*}{3}\sqrt{R_1 d^3}. \tag{8}$$

If we choose a radius

$$R_1 = R/2, \tag{9}$$

then the equations (7) and (8) coincide exactly with the Hertzian theory. The rule (9) means that the cross-section of the three-dimensional profile is stretched by the factor of 2 in the vertical direction.

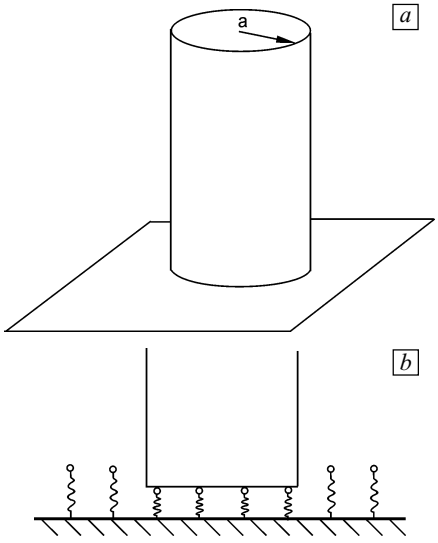

Fig. 1. Contact of a rigid cylindrical indenter with an elastic half-space (*a*) and its one-dimensional representation (*b*)

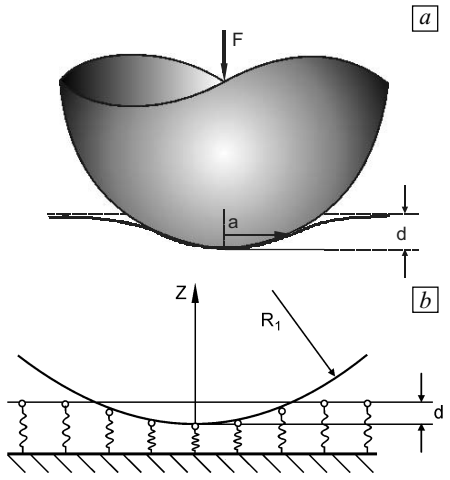

Fig. 2. Contact of a spherical indenter with a half-space (*a*) and its one-dimensional representation (*b*)

Hess showed that the exact mapping of contact problems to one-dimensional elastic foundations is possible for arbitrary bodies of revolution [6]. If a body of revolution is described by the equation

$$z(r) = \sum_{n=1}^{\infty} z_n(r) = \sum_{n=1}^{\infty} c_n r^n, \tag{10}$$

then a one-dimensional profile in a contact with an elastic foundation defined by (3) will have exactly the same contact properties as the original three-dimensional contact, provided that the profile is modified according to the following Hess rule:

$$z(r) = \sum_{n=1}^{\infty} c_n r^n \Rightarrow z_n(x) = \sum_{n=1}^{\infty} \tilde{c}_n x^n \tag{11}$$

with

$$\tilde{c}_n = \kappa_n c_n,\ \kappa_n = \frac{\sqrt{\pi}}{2}\frac{n\Gamma(n/2)}{\Gamma(n/2+1/2)}. \tag{12}$$

where $\Gamma(n)$ is the Gamma-function:

$$\Gamma(n) = \int_0^{\infty} t^{n-1} e^{-t} \mathrm{d}t. \tag{13}$$

In the Table 1, several values of κ_n are presented. In particular, for a cone (n = 1) we get $\kappa_1 = \pi/2$. Note that the power n is an arbitrary positive number (it must not to be an integer).

The general reason for the possibility of mapping three-dimensional contacts with bodies of revolution into one-dimension ones is simple, and it is instructive to discuss it. Let us consider a rigid indenter having the form

$$z(r) = c_n r^n, \tag{14}$$

which is pressed to a depth d into an elastic half-space. The unit of the coefficient c_n is $[m]^{1-n}$. As the equilibrium equations of elasticity do not contain any quantities with the dimension of length, it follows from dimensional analysis that the contact radius a can only be a function of the indentation depth of the form

$$a \propto c_n^{\alpha} d^{1-\alpha(1-n)}, \tag{15}$$

with an arbitrary constant exponent α. On the other hand, if the profile (14) is stretched in the horizontal plane by a factor of C ($r = r'C$) and at the same time in the vertical direction by the factor of C^n ($z = z'C^n$), then the profile does not change at all. The contact radius in the new coordinates scales as C^{-1} and the indentation depth remains unchanged. From Eq. (15), it follows that $C^{-1} = C^{\alpha n}$ and $\alpha = -1/n$. Thus, the contact radius should be a power function of the indentation depth of the form

$$a \propto (d/c_n)^{1/n}. \tag{16}$$

Once the dependence of the contact radius on the indentation depth is known, the dependence of the normal force follows straightforwardly. Indeed, the differential contact stiffness depends only on the current configuration of the contact and is given by the same equation as for a cylindrical indenter (see [3] or [7] for the proof):

$$\frac{\partial F_N}{\partial d} = 2aE^*. \tag{17}$$

With (16), it follows that

$$F_N \propto \frac{2E^*}{(1+1/n)} c_n^{-1/n} d^{1+1/n}. \tag{18}$$

In the one-dimensional case, it is trivially to see that both equations (16) and (17) remain valid. Thus, the power law (18) is valid as well, and it is only the question of the correct vertical scaling to get the results exactly equivalent.

Table 1

n	1	2	3	4	5	6	7	8	9	10
κ_n	1.571	2	2.356	2.667	2.945	3.2	3.436	3.657	3.866	4.063

3.1. Stress distribution in the contact area

Hess further found that the pressure distribution in a real three-dimensional contact can be reconstructed from the linear force density $q(x) = \Delta f(x)/\Delta x$, where $\Delta f(x)$ is the normal force in a spring having coordinate x. According to Hess, the pressure distribution is given by the Abel transformation [6]:

$$\sigma_{zz} = \frac{1}{\pi}\int_r^{\infty} \frac{q'(x)}{\sqrt{x^2 - r^2}} \mathrm{d}x. \tag{19}$$

For example, in the case of a cylindrical indenter, the force density $q(x)$ is constant inside the contact interval:

$$q(x) = \begin{cases} F_N/(2a) & \text{for } |x| < a, \\ 0 & \text{for } |x| > a. \end{cases} \tag{20}$$

Therefore, $q'(x) = \frac{F_N}{2a}(\delta(x+a) - \delta(x-a))$ and integral (19) gives

$$\sigma_{zz} = \frac{1}{\pi}\frac{F_N}{2a}\int_r^{\infty} \frac{\delta(x+a) - \delta(x-a)}{\sqrt{x^2 - r^2}} \mathrm{d}x = \\ = \begin{cases} \dfrac{F_N}{2\pi a^2}\dfrac{1}{\sqrt{1-(r/a)^2}} & \text{for } |r| < a, \\ 0 & \text{for } |r| > a, \end{cases} \tag{21}$$

which is exactly the stress distribution in a three-dimensional contact with a cylindrical indenter of radius a (see, e.g., [8]). Similarly, for the parabolic case, the force density in the one-dimensional case is calculated trivially to be

$$q(x) = E^*(d - x^2/(2R_1)) \text{ for } |x| < a = \sqrt{2R_1 d}. \tag{22}$$

For the derivative, we get $q'(x) = E^* x/R_1$. Substitution into (19) gives

$$\sigma_{zz} = \frac{E^*}{\pi R_1}\int_r^{\infty} \frac{x\mathrm{d}x}{\sqrt{x^2 - r^2}} = \frac{E^*}{\pi R_1}\int_r^{a} \frac{x\mathrm{d}x}{\sqrt{x^2 - r^2}} = \\ = \frac{2}{\pi}E^*\left(\frac{d}{R}\right)^{1/2}\sqrt{1-(r/a)^2}, \tag{23}$$

which is exactly the result for the Hertzian problem.

Equation (19) gives the exact stress distribution, not only in these simple classic cases but for arbitrary bodies of revo-

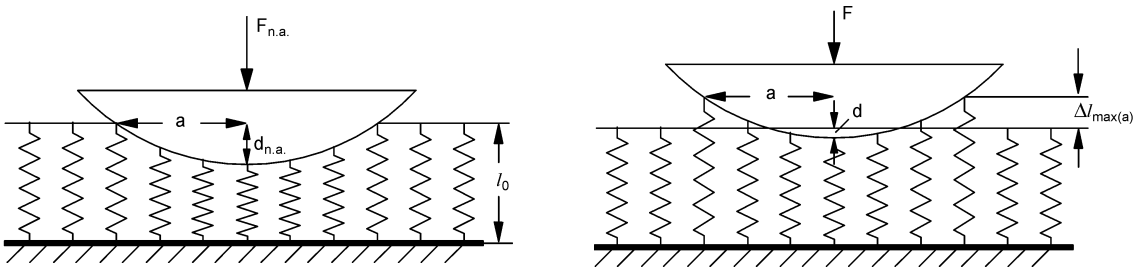

Fig. 3. Adhesive contact during the pressing and detaching phases

lution, provided the Hess rule has been applied for modification of the profile. Exact proof of this statement can be found in [6].

3.2. Normal contacts with adhesion

Hess succeeded in generalizing the reduction method to adhesive contacts. His argument was very simple and elegant: It is known that the stress distribution in an adhesive contact described by the JKR-theory [9] is a superposition of a pressure distribution with a parabolic indenter and a negative stress distribution by "rigid pulling" the contact area. As both of these contact problems can be mapped exactly into one dimension, this should be valid for the entire adhesive problem as well. The Hess rule for adhesive contacts is the following: If we first press a modified indenter (11) into the elastic foundation and then pull it off as shown in Fig. 3, then the springs will detach when the following critical elongation is achieved [6, 10]:

$$\Delta l_{\max}(a) = \sqrt{\frac{2a\pi\gamma_{12}}{E^*}}. \tag{24}$$

Note that this criterion is non-local, as it depends on the actual radius of the contact region.

As a simple example let us consider an adhesive contact between a rigid cylinder with a radius a and an elastic half-space (Fig. 4). In this case, all springs will detach at the instant in which all of them achieve the critical elongation (24). The total normal force which must be applied to achieve this state is just

$$F_A = 2aE^*\sqrt{\frac{2a\pi\gamma_{12}}{E^*}} = \sqrt{8E^*a^3\pi\gamma_{12}}, \tag{25}$$

which is the exact result for this adhesive problem [6]. Similar calculations for a parabolic profile would lead to the classical JKR-result $F_A = 3/2\,\pi R\gamma_{12}$. Application of Hess rule (24) provides not only exact adhesive forces for an arbitrary body of revolution but also the complete force-displacement dependence and force-contact radius dependence. The proof can be found in [6].

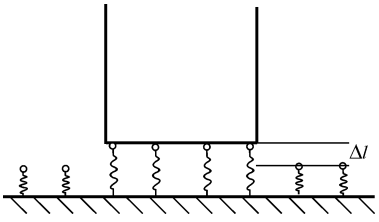

Fig. 4. The one-dimensional equivalent system for the adhesive contact between a rigid cylinder and an elastic half-space

4. Tangential contact

In this section, we would like to illustrate the application of the method of reduction of dimensionality using an example of a tangential contact with friction. A parabolic body is initially pressed into an elastic half-space with the normal force F_N and subsequently tangentially loaded with a force F_x (Fig. 5). It is assumed that the friction between the bodies can be described using the simple Coulomb's law of friction with a constant coefficient of friction. Due to the fact that at the edges of the contact area, the normal force in the springs disappears, a sliding domain exists here, while in the center of the contact area, as long as the tangential force is not too large, the surfaces stick. We denote the radius of the sticking domain with c.

The vertical displacement of a spring at a distance x from the center of the contact is

$$u_z(x) = d - \frac{x^2}{2R_1} \tag{26}$$

and the resulting spring force is

$$f_N(x) = E^* u_z(x)\Delta x = \left(d - \frac{x^2}{2R_1}\right)E^*\Delta x. \tag{27}$$

The contact radius is determined from the condition $u_z(a) = 0$ and, according to this, is equal to

$$a = \sqrt{2R_1 d}. \tag{28}$$

We denote the horizontal displacement of the parabolic indenter relative to the substrate as u_x. Then, the force acting on a spring which sticks to the substrate is equal to

$$f_x(x) = \Delta k_x u_x = G^*\Delta x u_x. \tag{29}$$

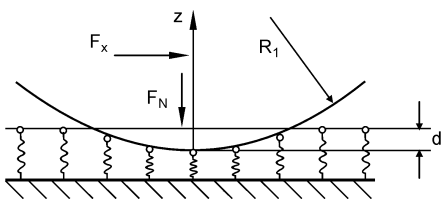

Fig. 5. Tangential contact with friction with a parabolic body

The boundaries of the sticking region are determined from the condition that the tangential force reaches the maximum possible value for the static friction force:

$$f_x(c) = \mu f_N(c) \tag{30}$$

or

$$G^* \Delta x u_x = \mu \left(d - \frac{c^2}{2R_1} \right) E^* \Delta x. \tag{31}$$

From this, it follows that

$$c^2 = 2R_1 \left(d - \frac{G^*}{E^*} \frac{u_x}{\mu} \right). \tag{32}$$

Solving for u_x results in

$$u_x = \mu \frac{E^*}{G^*} \left(d - \frac{c^2}{2R_1} \right). \tag{33}$$

The sliding in the remaining regions means that Coulomb's law of friction is fulfilled in these regions:

$$f_x(c) = \mu f_N(c), \text{ if } c < |x| < a. \tag{34}$$

We now calculate the normal and tangential forces in this state. The normal force results in the Hertzian result:

$$F_N = \int_{-a}^{a} \left(d - \frac{x^2}{2R_1} \right) E^* \mathrm{d}x =$$

$$= \frac{4}{3} E^* (2R_1)^{1/2} d^{3/2} = \frac{2E^* a^3}{3R_1}. \tag{35}$$

The tangential force is calculated as

$$F_x = 2\int_0^c G^* u_x \mathrm{d}x + 2\int_c^a \mu \left(d - \frac{x^2}{2R_1} \right) E^* \mathrm{d}x =$$

$$= \frac{2E^* a^3 \mu}{3R_1} \left(1 - \left(\frac{c}{a} \right)^3 \right) = \mu F_N \left(1 - \left(\frac{c}{a} \right)^3 \right). \tag{36}$$

From this, the relationship from the three-dimensional calculation results [3]:

$$\frac{c}{a} = \left(1 - \frac{F_x}{\mu F_N} \right)^{1/3}. \tag{37}$$

The maximum displacement until the point of complete sliding is given by (33) through the insertion of $c = 0$:

$$u_{x,\max} = u_x = \mu \frac{E^*}{G^*} d \tag{38}$$

and is likewise identical to the three-dimensional results.

It can be easily shown that the Abel transformation (19) provides the correct stress distribution in a true three-dimensional tangential contact also in this case. The (tangential) force density is given in this case by the following relations:

$$q_x(x) = \begin{cases} \mu \left(d - \dfrac{x^2}{2R_1} \right) E^* \text{ for } c < |x| < a, \\ G^* u_x \text{ for } |x| < c, \\ 0 \text{ for } |x| > a. \end{cases} \tag{39}$$

In the sticking part of the contact, the force density is constant and can be represented as the difference between two force functions $q_x(x) = q_1(x) - q_2(x)$, where

$$q_1(x) = \mu E^* \left[d - \frac{x^2}{2R_1} \right] = \frac{\mu E^*}{2R_1} (a^2 - x^2),$$

$$q_1(x) = \mu E^* \left[\left(d - \frac{G^* u_x}{E^* \mu} \right) - \frac{x^2}{2R_1} \right] = \frac{\mu E^*}{2R_1} (c^2 - x^2). \tag{40}$$

From this, it follows immediately that the three-dimensional stress distribution will be a difference between two "Hertzian-like" stress distributions, which is really the case in a true three-dimensional system [3]. Thus, the tangential contact with friction is exactly mapped to the one-dimensional system. It can be shown that this is valid for arbitrary bodies of revolution.

5. Viscoelastic contacts and thermal effects

For viscoelastic bodies such as rubber, the contact can be seen as quasi-static when the penetration velocity and the sliding velocity are smaller than the smallest speed of sound (which corresponds to the smallest modulus of elasticity). If this condition is met and an area of an elastomer is excited at a frequency ω, then there is a linear relation between the force and displacement with stiffness that is proportional to the contact radius. Hence, this system can also be presented using a one-dimensional system, where the stiffness of the individual springs must be chosen according to (3). Rubber can be considered to be an incompressible medium so that $\nu = 1/2$ and for a contact between a rigid indenter and a rubber half-space, the stiffness must be chosen to be

$$\Delta k_z = E^*(\omega) \Delta x = \frac{E(\omega)}{1 - \nu^2} \Delta x =$$

$$= \frac{2G(\omega)}{1 - \nu} \Delta x = 4G(\omega) \Delta x. \tag{41}$$

The corresponding relation for forces in the time domain reads

$$f_z(t) = 4\Delta x \int_{-\infty}^{t} G(t - t') \dot{z}(t') \mathrm{d}t', \tag{42}$$

where $G(t)$ is the time dependent shear modulus [3].

For tangential contacts the stiffness must be chosen according to (6):

$$\Delta k_x = G^*(\omega) \Delta x = \frac{4G(\omega)}{2 - \nu} \Delta x \approx \frac{8}{3} G(\omega) \Delta x. \tag{43}$$

The corresponding force relation in the time domain reads

$$f_x(t) = \frac{8}{3} \Delta x \int_{-\infty}^{t} G(t - t') \dot{z}(t') \mathrm{d}t'. \tag{44}$$

The validity of the mapping of three-dimensional contacts onto one-dimensional viscoelastic foundation is further based on the equivalence of surface profiles for all media with linear rheology at a given indentation. Let us illustrate this important topic by comparing the indentation

of an elastic and a viscous medium. The surface profile is determined unambiguously by the equilibrium equation of the medium and the (linear) stress relation on the surface. For an elastic medium, the equilibrium relation reads

$$G\Delta\mathbf{u} + (\lambda + G)\nabla(\nabla \cdot \mathbf{u}) = 0, \tag{45}$$

where $\lambda = 2\nu G/(1-2\nu)$ is the first Lame coefficient [11]. The corresponding "equilibrium equation" for a linearly viscous fluid is the Navier–Stokes equation without inertia terms [12]:

$$\eta\Delta\dot{\mathbf{u}} + (\xi + \eta)\nabla(\nabla \cdot \dot{\mathbf{u}}) = 0. \tag{46}$$

In the case of an elastic continuum, the stress is a linear function of the gradients of the displacement field **u**, while in the case of a fluid, the same is valid for the gradient of the velocity field $\dot{\mathbf{u}}$. The same form of equations (after substitution of the displacement field with the velocity field) implies that all relations which are valid at a given contact configuration for an elastic continuum for force-displacement relations will be valid for a viscous medium for force-velocity relations. The incremental changes in contact configuration and indentation depth do not depend on elastic properties of the medium[1]. This leads straightforwardly to the conclusion that at the given indentation depth, the configurations of an elastic and of a viscous medium are strictly identical. This is valid not only for rotationally symmetric profiles, but for arbitrary profiles, however, only during the indentation phase. It was first Radok who found this property and used it for developing the contact mechanics of viscoelastic media [13].

Finally, let us note that the stationary equation of thermal conductivity

$$\Delta T = 0 \tag{47}$$

(Δ is the Laplace operator here and in equations (45) and (46)) is of the same form as the equations of elasticity (45) and for fluid dynamics (46). The same is valid for equations of electrical conductivity. This leads to a close connection between the elastic properties and some electrical and thermal properties [14]. For example, the electrical contact conductance Λ is linearly proportional to the incremental stiffness:

$$k = \frac{\partial F_N}{\partial d} = E^*(\rho_1 + \rho_2)\Lambda/2,$$

where ρ_1 and ρ_2 are the resistivities of the contacting bodies [14]. Electrical and thermal properties can, therefore, be integrated into the method of reduction of dimensionality in a natural and simple way.

6. Adhesion with viscoelastic contacts

For improved understanding of the phenomenon of adhesion and to be able to transfer the classical results to viscoelastic media, it is advantageous to obtain a picture of the microscopic structure of an adhesive contact. We consider an adhesive contact between a flat, rigid stamp and an elastic body (Fig. 6, *a*). As the stamp is drawn away with the force *F* in the upward direction, the following pressure distribution arises in the contact area [3]:

$$p = -p_0\left(1 - \left(\frac{r}{a}\right)^2\right)^{-1/2} \tag{48}$$

with

$$p_0 = \frac{F}{2\pi a^2}. \tag{49}$$

Near the edge of the contact area, $r = a - \Delta r$, with $\Delta r \ll a$, the distribution has a singularity of the form

$$p = p_0\sqrt{\frac{a}{2\Delta r}}. \tag{50}$$

In the end, this singularity is the physical reason for the severing of the adhesive bonds between the bodies [15, 16]. For the global equilibrium, only the form of this singularity is important. The pressure distribution far away from the crack tip plays no role in the equilibrium. Because of the molecular structure, the singularity (50) does not exist in reality. The pressure reaches a high, but finite, maximum on the order of magnitude of

$$p_{\max} \approx p_0\sqrt{\frac{a}{2b}}, \tag{51}$$

where *b* can be interpreted as the characteristic molecular size in the simplest case. In general, *b* is of the order of magnitude of the "process zone" at the crack tip [17].

The severing of molecular bonds near the edge of an adhesive contact occurs if a certain threshold is surpassed. In the elastic case, it is unimportant whether we take the critical strain, critical stress, or critical work, because in this case, all three are explicitly linked to one another. In the case of a contact with an elastomer, this is no longer the case, due to the fact that in such materials, the stress is not a distinct function of strain, but rather is dependent also on the rate of strain. Therefore, in this case various "failure criteria" are possible, from which we will discuss two in the following.

6.1. Deformation criterion

The stress in Eq. (51) leads to a local deformation in the medium of the order of magnitude of

$$\varepsilon_{\max} \approx \frac{p_{\max}}{E^*} = \frac{p_0}{E^*}\sqrt{\frac{a}{2b}}. \tag{52}$$

Assume that the adhesive contact is lost when the relative displacement of the "contacting molecules" in the vertical direction reaches a critical value b_c. We can then rewrite the approximation (52) in the following form:

$$\varepsilon_{\max} \approx \frac{b_c}{b} \approx \frac{p_0}{E^*}\sqrt{\frac{a}{2b}}. \tag{53}$$

[1] This is seen very clearly in the fact that the contact radius in the Hertz problem $a = \sqrt{Rd}$ does not depend on elastic moduli.

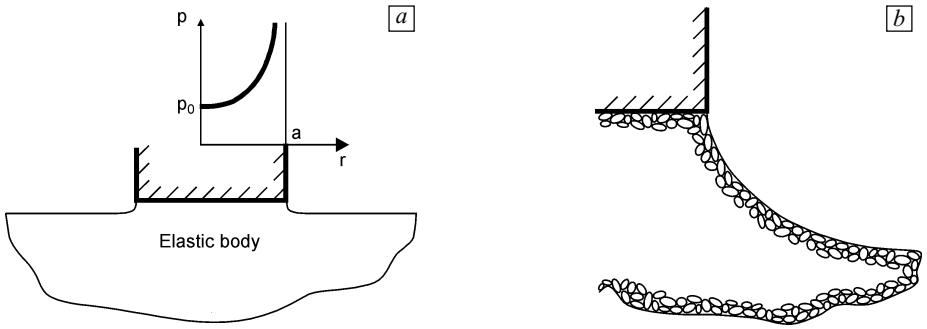

Fig. 6. Adhesive contact of an elastic body with a flat stamp (*a*); enlarged representation of the "crack tip" (the region in direct proximity to the contact boundary) (*b*)

From this, the following value of p_0 is obtained:

$$p_0 \approx E^* \sqrt{\frac{2b}{a}} \frac{b_c}{b}. \tag{54}$$

The resulting force of adhesion is

$$F_A = 2^{3/2} \pi E^* b_c b^{-1/2} a^{3/2}. \tag{55}$$

For the critical vertical displacement of the entire stamp, we obtain

$$u_A = \frac{F_A}{2aE^*} = 2^{1/2} \pi b_c b^{-1/2} a^{1/2}. \tag{56}$$

By introducing the definition

$$b^* = 2\pi^2 b_c^2 / b \tag{57}$$

(b^* is a constant with the unit of length and is on the order of magnitude of the length of the polymer molecule in the elastomer), we can write (56) in the form

$$u_A = \sqrt{b^* a}. \tag{58}$$

Notice that this equation does not contain the modulus of elasticity; it is valid in the same form also for arbitrary media with linear rheology, providing that the assumed deformation criterion for the fracture is maintained. For elastomers with the deformation fracture criterion, the Hess law (24) must be replaced with

$$\Delta l_{\max}(a) = \sqrt{b^* a}. \tag{59}$$

6.2. Stress criterion

Other criteria are conceivable. For example, the contact can be severed when the stress maximum (51) reaches a critical value of σ_c:

$$p_{\max} \approx p_0 \sqrt{\frac{a}{2b}} = \sigma_c. \tag{60}$$

Because the relationship (49) is universally valid for all media with a linear rheology, we obtain the following force of adhesion:

$$F_A = 2\pi a^2 p_0 = 2^{3/2} \pi a^{3/2} b^{1/2} \sigma_c. \tag{61}$$

With this criterion, the dependence of the force of adhesion on the radius of the stamp is the same as in the JKR-model and the force of adhesion is independent from the rate of displacement. The Hess law is formulated in this case not for the strain in individual springs, but for the force $\Delta f_{x,\max} / \Delta x = F_A / (2a)$:

$$\frac{\Delta f_{x,\max}}{\Delta x} = \pi \sigma_c \sqrt{2ab}. \tag{62}$$

7. Normal contacts with rough surfaces

An important question is whether the method of reduction of dimensionality is restricted to the bodies of revolution or can be applied to a broader class of surface topographies, first of all to the contact of rough surfaces. The importance of roughness was first stressed by Bowden and Tabor [1]. It was a hot topic in the 50s and 60s during the 20th century [18, 19] and remains an important research topic until now [20–24]. Numerical simulations of contacts between rough surfaces cost very much computation time this is one of the main reasons why numerical simulation methods are not used until now in engineering tribology. We will show below in this section that there are empirical and theoretical reasons to state that the method of reduction of dimensionality is applicable at least to randomly rough fractal surfaces as well, thus, providing a practical tool for rapid simulation of contact problems. The validity of this hypothesis was first studied in [5].

In order to cross over to a contact between bodies with rough surfaces, a rule for the production of a one-dimensional profile, which is equivalent to the three-dimensional body in a contact mechanical sense, must be formulated. As the motivation for this replacement, we use a few ideas from the Greenwood–Williamson model [19]. The results and quality of the replacement system, however, prove to be much better than the Greenwood–Williamson model itself.

In the model of Greenwood and Williamson, the individual contacts are considered to be independent from each other. Under these conditions, only the distribution of the heights of the asperities and the radii of curvature play a role. So, our goal is first to generate a one-dimensional system, which has the necessary statistical distributions of heights and radii of curvature.

To simplify matters, we assume that the topographies of both the two-dimensional surface (of a three-dimensional body) and of its one-dimensional mapping can be unambiguously characterized by their power spectra $C_{2D}(\mathbf{q})$ and $C_{1D}(q)$, which are defined according to

$$C_{2D}(\mathbf{q}) = \frac{1}{(2\pi)^2}\int\langle h(\mathbf{x})h(\mathbf{0})\rangle e^{-i\mathbf{q}\cdot\mathbf{x}}\mathrm{d}^2x \quad \text{for a surface,}$$
$$C_{1D}(q) = \frac{1}{2\pi}\int\langle h(x)h(0)\rangle e^{-iqx}\mathrm{d}x \quad \text{for a line,} \tag{63}$$

where $h(\mathbf{x})$ is the height profile taken from the average so that $\langle h\rangle = 0$; $\langle . \rangle$ means averaging over the statistical ensemble. Furthermore, we assume that the surface topography is statistically homogeneous and isotropic. Under these conditions, the power spectrum $C_{2D}(\mathbf{q})$ is only dependent on the magnitude q of the wave vector $\mathbf{q}$.

Many technically relevant surfaces are fractal self-affine surfaces [2]. These surfaces have a spectral density obeying a power law:

$$C_{2D}(q) = \text{const}\cdot\left(\frac{q}{q_0}\right)^{-2H-2} \quad \text{for a surface,}$$
$$C_{1D}(q) = \text{const}\cdot\left(\frac{q}{q_0}\right)^{-2H-1} \quad \text{for a line,} \tag{64}$$

where H is the Hurst exponent ranging from 0 to 1 [2]. It is directly related to the fractal dimension of an original two-dimensional surface $D_f = 3 - H$.

The surface topography is calculated with the help of the power spectrum according to

$$h(\mathbf{x}) = \sum_{\mathbf{q}} B_{2D}(\mathbf{q})\exp(i(\mathbf{q}\cdot\mathbf{x} + \phi(\mathbf{q}))),$$
$$B_{2D}(\mathbf{q}) = \frac{2\pi}{L}\sqrt{C_{2D}(\mathbf{q})} = \overline{B}_{2D}(-\mathbf{q}) \tag{65}$$

for two-dimensional surfaces and with

$$h(x) = \sum_{q} B_{1D}(q)\exp(i(qx + \phi(q))),$$
$$B_{1D}(q) = \sqrt{\frac{2\pi}{L}C_{1D}(q)} = \overline{B}_{1D}(-q) \tag{66}$$

for one-dimensional lines, with random phases $\phi(\mathbf{q}) = -\phi(\mathbf{q})$ on the interval $[0, 2\pi)$.

In order to produce a one-dimensional system with the same contact properties as the three-dimensional system, the one-dimensional power spectrum must be used according to the rule

$$C_{1D}(q) = \pi q C_{2D}(q). \tag{67}$$

Qualitative arguments for this rule are the following: The averages of the squares of the heights for the two-dimensional and one-dimensional cases, respectively, are

$$\left\langle h^2\right\rangle_{2D} = 2\pi\int_0^\infty qC_{2D}(q)\mathrm{d}q, \tag{68}$$

$$\left\langle h^2\right\rangle_{1D} = 2\int_0^\infty C_{1D}(q)\mathrm{d}q. \tag{69}$$

They are the same when $C_{1D}(q) = \pi q C_{2D}(q)$. The corresponding root mean squares of the surface gradient $\langle\nabla z^2\rangle$ and curvature $\langle\kappa^2\rangle$ also coincide in this case[1]. Note that the Hurst exponents of both one- and two-dimensional surfaces coincide as well. This last property is very important and allows an analytical substantiation for the applicability of the method of reduction of dimensionality to randomly rough surfaces to be given.

Let us illustrate the applicability of the method of reduction of dimensionality using the example of normal stiffness of bodies with rough surfaces. Stiffness of fractally rough surfaces without long wavelength cut-off has been investigated in [24]. Consider a cylindrical rigid indenter with diameter $L = 2a$ having a self-affine fractal surface described by (64). If it is pressed into an elastic half-space, first the tallest peak comes into contact and finally, at very large normal force, complete contact will be achieved. In this final state, the contact stiffness is equal to $k_{z,\max} = E^* L$. Now, we undertake the transformation (67) of the surface power spectrum and generate a rough line according to the rule (66) having the length L. This choice of length guarantees automatically that the maximum stiffness at the complete contact will exactly coincide for three- and one-dimensional cases. Furthermore, we concentrate our attention to the region of small forces and incomplete contact. It was shown in [24] that there are several rigorous scaling relations which the dependence of contact stiffness k_N and the normal force must fulfill. These scaling relations lead to the following general form of the stiffness-force dependence, both for the one- and three-dimensional case:

$$\frac{k_N}{E^* L} = \zeta\left(\frac{F}{E^* hL}\right)^\alpha, \tag{70}$$

where α is a constant exponent and ζ is a constant coefficient; both of them may only depend on the Hurst exponent.

There are analytical considerations supporting the power law dependence of the contact stiffness and the strict equivalence of three-dimensional and one-dimensional results for small fractal dimensions. For fractal surfaces without long wavelengths cut-off, the surface has a pronounced non-planarity on the largest scale. Therefore, the contact at small contact force is localized in the vicinity of only one point of apparent contact area. Now, let us make the following transformation of the surface:

$$L' = CL,\ h' = C^H h,\ d' = d. \tag{71}$$

According to the definition of a self-affine surface, this transformation provides the same surface (or a surface with the same statistical properties) — as long as the real contact spot is inside the initial size of the system. This means that the transformation (71) lets the complete "contact state," including the contact force and contact stiffness (defined

[1] For two-dimensional cases, we define $\kappa^2 = \kappa^{(1)}\kappa^{(2)}$, where $\kappa^{(1)}$ and $\kappa^{(2)}$ are the principal radii of curvature of the surface.

as $\partial F/\partial d$), remain unchanged:

$$F' = F,\ k' = k. \tag{72}$$

Substitution of the transformations (71) and (72) into (70) gives

$$\alpha = 1/(1+H). \tag{73}$$

These arguments do not depend on the dimensionality of the system and are valid for both the initial three-dimensional contact and its one-dimensional mapping. The constants ζ may, of course, be different, but can easily be adjusted — just as in the case of simple rotationally of symmetric bodies — with a universal scaling factor, which depends only on the Hurst exponent and must be determined once empirically with large-scale direct simulations. This has already been done in [25].

The method of reduction of dimensionality, thus, produces exact limiting dependences of the contact stiffness of self-affine fractal surfaces too — both in the limit of very small and very large loads.

8. Force of friction

Friction between rough solid surfaces is of considerable importance in many applications. In the present paper we confine ourselves only to the consideration of friction between a rigid rough surface and an elastomer with linear rheology. As discussed above, the force-displacement relations in this case are described correctly by the method of reduction of dimensionality. We will illustrate this with two examples. Grosch first established that the friction of elastomers is determined by the internal losses in contacting bodies and is, hence, closely related to the rheology of these materials [26]. Simple analytical estimations [3] show that the coefficient of friction between an elastomer and a rough solid surface obeys the following relation:

$$\mu = \xi \nabla z \frac{G''(kv)}{|\hat{G}(kv)|}, \tag{74}$$

where ∇z is the mean square slope (gradient) of the solid surface profile $z = z(x, y)$; $\hat{G}(\omega)$ is the frequency dependent complex shear modulus of the elastomer; $G''(\omega)$ is the imaginary part of this complex quantity; k is the characteristic wave vector of the solid surface profile; v is the relative velocity of sliding; ξ is a dimensionless constant on the order of unity and $|\hat{G}(\omega)|$ is the absolute value of the complex shear modulus. Since equation (74) is derived on the basis of qualitative considerations, the exact value of a constant ξ is unknown and can only be determined by means of exact numerical simulations.

Relation (74) acquires a simpler form, provided that the complex shear modulus is purely imaginary (or its imaginary part is much greater than the real part). Then, the ratio $G''(\omega)/|\hat{G}(\omega)|$ is unity and (74) reduces to

$$\mu = \xi \nabla z. \tag{75}$$

In [27], it was proven by direct numerical simulation that this relation is valid for fractal surfaces with the coefficient ξ being approximately 1.

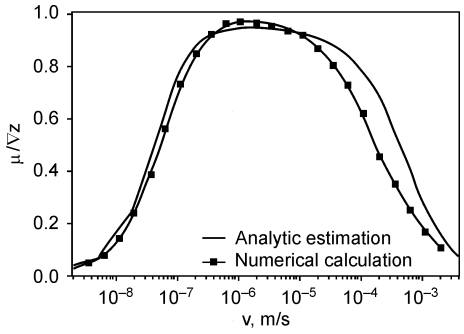

Fig. 7. Dependence of the friction coefficient for a contact of a two-dimensional rough, non-fractal surface with a half-space having the linear rheological law (76). The solid line is estimation (74) and the dots, the numerical simulation using the method of reduction of dimensionality

The more general relation (74) was validated in [28]. There, the time dependent modulus of the form

$$G(t) = G_0 + G_1\tau_1 \int_{\tau_1}^{\tau_2} \tau^{-s} e^{-t/\tau} \mathrm{d}\tau \tag{76}$$

has been used with $G_0 = 1$ MPa, $G_1 = 1$ GPa, $\tau_1 = 10^{-2}$ s, $\tau_2 = 10^2$ s and $s = 2$. This dependency is characterized by a broad spectrum of relaxation times ranging from 10^{-2} to 10^2 s. The results of numerical simulation using the force rule (42) is presented together with the analytical estimation (74) in Fig. 7. One can see that the numerical simulation reproduces the three-dimensional estimation very well. However, as there are no exact three-dimensional calculations for the force of friction, it is not possible to decide if the small discrepancy is due to the inaccuracy in the one-dimensional numerical simulation or to the inaccuracy in the three-dimensional estimation.

9. Discussion

The described method of reduction of dimensionality maps a three-dimensional contact problem to one of one dimension. This leads to a drastic reduction in the computation time and simplification of analytical calculations. The reduction which is achieved by this method is two-fold: First, a system, whose degrees of freedom correspond to a three-dimensional space, is replaced by a system with the same linear size, whose degrees of freedom correspond to a one-dimensional space. The second, equally important reduction is that a system with interacting degrees of freedom is replaced by a system with independent degrees of freedom. This property opens the possibility of further reduction of calculation time by parallel processing of independent degrees of freedom. A possibility of such replacement seems at first glance miraculous, but was rigorously proved for at least two classes of surface topographies: (i) for arbitrary bodies of revolution and (ii) for randomly rough fractal self-

affine surfaces. The mapping is no approximation, but is exact. The time reduction for realistic systems of technical interest is at least six decimal orders of magnitude, thus, opening completely new possibilities in numerical simulation of contacts with real topography. In particular, it becomes possible to incorporate the microscopic simulations directly (in each time step) into a macroscopic simulation of the system dynamics and, thus, really to close the gap between the micro- and macroworld for many classes of tribological problems.

The applicability of the method is, of course, restricted to the scales where macroscopic continuum mechanics can be used. This means that the smallest, atomic scale cannot be incorporated into the method directly. However, it is possible to summarize the interactions on the smallest scale to a phenomenological friction, which must be introduced additionally as an empirical frictional law. As a matter of fact, that is what we all do by using the notion of the force of friction: What we call the force of friction is nothing but an empirical simplification of all microscopical interactions which we cannot describe explicitly. With this notion, a distinction of micro- and macroscale is always associated (however, mostly implicitly). In [29], it was shown that the boundary between macro- and microdescription can be moved continuously in a sort of renormalization group, which gives different laws of friction at different scales. What the method of reduction of dimensionality really does is shifting this boundary between micro and macro to the smallest possible scale, at which a mechanical description of a material fails. It is interesting to analyze, whether it is principally possible to introduce on the smallest scale interactions of the type of Prandtl–Tomslinson model [30] or its extensions for boundary lubrication [31], thus, providing a link between the macroscopic tribology and atomic scale tribology [32]. All of these topics are matter for future research.

I am grateful to my colleagues A. Dimaki, A.E. Filippov, T. Geike, M. Heβ, R. Pohrt, and S.G. Psakhie for many valuable discussions of the fundamentals of the method of reduction of dimensionality and its extensions. I acknowledge financial support of this research by the Deutsche Forschungsgemeinschaft in the framework of several projects.

References

[1] F.P. Bowden and D. Tabor, The Friction and Lubrication of Solids, Clarendon Press, Oxford, 1986.
[2] B.N.J. Persson, Contact mechanics for randomly rough surfaces, Surf. Sci. Rep., 61, No. 201–227 (2006).
[3] V.L. Popov, Contact Mechanics and Friction. Physical Principles and Applications, Springer-Verlag, Berlin, 2010.
[4] V.L. Popov and S.G. Psakhie, Numerical simulation methods in tribology, Tribol. Int., 40 (2007) 916.
[5] T. Geike and V.L. Popov, Mapping of three-dimensional contact problems into one dimension, Phys. Rev. E, 76 (2007) 036710.
[6] M. Heβ, Über die exakte Abbildung ausgewählter dreidimensionaler Kontakte auf Systeme mit niedrigerer räumlicher Dimension, Cuvillier-Verlag, Göttingen, 2011.
[7] I.N. Sneddon, The relation between load and penetration in the axisymmetric Boussinesq problem for a punch of arbitrary profile, Int. J. Eng. Sci., 3 (1965) 47.
[8] K.L. Johnson, Contact Mechanics, Cambridge University Press, Cambridge, 1987.
[9] K.L. Johnson, K. Kendall, and A.D. Roberts, Surface energy and the contact of elastic solids, Proc. Roy. Soc. Lond. A. Math., 324 (1971) 301.
[10] M. Heβ, On the reduction method of dimensionality: The exact mapping of axisymmetric contact problems with and without adhesion, Phys. Mesomech., 15, No. 5–6 (2012) 264.
[11] L.D. Landau and E.M. Lifschitz, Lehrbuch der Theoretischen Physik. Band 7. Elastizitätstheorie, Akademie-Verlag, Berlin, 1965.
[12] L.D. Landau and E.M. Lifschitz, Lehrbuch der Theoretischen Physik. Band 6: Hydrodynamik, Akademie-Verlag, Berlin, 1991.
[13] J.R.M. Radok, Viscoelastic stress analysis, Q. Appl. Math., 15 (1957) 198.
[14] J.R. Barber, Bounds on the electrical resistance between contacting elastic rough bodies, Proc. Roy. Soc. Lond. A, 495 (2003) 53.
[15] A.A. Griffith, The phenomena of rupture and flow in solids, Philos. T. Roy. Soc. A, 221 (1921) 163.
[16] L. Prandtl, Ein Gedankenmodell für den Zerreißvorgang spröder Körper, J. Appl. Math. Mech., 13 (1933) 129.
[17] D. Maugis, Contact, Adhesion, and Rupture of Elastic Solids, Springer-Verlag, Berlin, 2000.
[18] J.F. Archard, Elastic deformation and the laws of friction, Proc. Roy. Soc. A, 243 (1957) 190.
[19] J.A. Greenwood and J.B.P. Williamson, Contact of nominally flat surfaces, Proc. R. Soc. A, 295 (1966) 300.
[20] S. Hyun and M.O. Robbins, Elastic contact between rough surfaces: Effect of roughness at large and small wavelengths, Tribol. Int., 40 (2007) 1413.
[21] C. Campana and M.H. Müser, Practical Green's function approach to the simulation of elastic, semi-infinite solids, Phys. Rev. B, 74 (2006) 075420.
[22] S. Akarapu, T. Sharp, and M.O. Robbins, Stiffness of contacts between rough surfaces, Phys. Rev. Lett., 106 (2011) 204301.
[23] C. Campana, B.N.J. Persson, and M.H. Müser, Transverse and normal interfacial stiffness of solids with randomly rough surfaces, J. Phys. Condens. Matt., 23 (2011) 085001.
[24] R. Pohrt and V.L. Popov, Normal contact stiffness of elastic solids with fractal rough surfaces, Phys. Rev. Lett., 108 (2012) 104301.
[25] R. Pohrt and V.L. Popov, Investigation of the dry normal contact between fractal rough surfaces using the reduction method, comparison to 3D simulation, Phys. Mesomech., 15, No. 5–6 (2012) 275.
[26] K.A. Grosch, The relation between the friction and viscoelastic properties of rubber, Proc. Roy. Soc. Lond. A. Mat., 274 (1963) 21.
[27] V.L. Popov and A.E. Filippov, Force of friction between fractal rough surface and elastomer, Tech. Phys. Lett., 36 (2010) 525.
[28] V.L. Popov and A.V. Dimaki, Using hierarchical memory to calculate friction force between fractal rough solid surface and elastomer with arbitrary linear rheological properties, Tech. Phys. Lett., 37 (2011) 8.
[29] A.E. Filippov and V.L. Popov, Fractal Tomlinson model for mesoscopic friction: From microscopic velocity-dependent damping to macroscopic Coulomb friction, Phys. Rev. E, 75 (2007) 027103.
[30] L. Prandtl, Ein Gedankenmodell zur kinetischen Theorie der festen Körper, J. Appl. Math. Mech., 8 (1928) 85.
[31] V.L. Popov, A theory of the transition from static to kinetic friction in boundary lubrication layers, Solid State Commun., 115 (2000) 369.
[32] E. Meyer, R.M. Overney, K. Dransfeld, and T. Gyalog, Nanoscience: Friction and Rheology on the Nanometer Scale, World Scientific, Singapore, 1998.